

# Modeling of the deuteron wave function in coordinate representation and calculations of polarization characteristics

V. I. Zhaba

*Uzhgorod National University, Department of Theoretical Physics,  
54, Voloshyna St., Uzhgorod UA-88000, Ukraine.*

Received 2 April 2020; accepted 14 October 2020

Modeling of the deuteron wave function in coordinate representation for the nucleon-nucleon potential Reid93 were performed. For this purpose, the asymptotics of the radial wave function near the origin of coordinates and at infinity are taken into account. The most simple and physical asymptotics were applied. In this case, the superfluous knots of both components of the deuteron wave function for the coordinate value  $r = 0.301$  fm were compensated. Taking into account the asymptotics of the wave function has little effect on the general behavior of the calculated polarization characteristics of  $t_{20}$  and  $A_{yy}$ . Particular points of the transmitted momentum have been identified, where the tensor deuteron polarization  $t_{20}$  and the tensor analyzing power  $A_{yy}$  show a clear difference.

*Keywords:* Deuteron; wave function; knot; tensor polarization; tensor analyzing power.

PACS: 03.65.Nk; 13.75.Cs; 13.40.Gp; 13.88; 21.45.Bc

DOI: <https://doi.org/10.31349/RevMexFis.67.137>

## 1. Introduction

The deuteron is a coupled system consisting of two nucleons (neutron and proton) [1, 2]. The cognitions about such a few body-nucleon system allows us to study the features of the deuteron behavior of both the two-particle system and the nucleon-nucleon interaction, taking into account various forms of potential models and approaches. The calculated theoretical values of polarization observables in processes with the participation of deuteron (electron-deuteron scattering, deuteron-proton scattering,  $A(d,d')X$  reactions on light nuclei, and others) can be compared with experimental data. Theoretical calculations of the polarization characteristics for such processes are based on the deuteron wave function (DWF) in coordinate representation.

On the one hand, the deuteron is fairly well studied both theoretically and experimentally. Static parameters have been reviewed and identified repeatedly. However, on the other hand, there are some inconsistencies and problems. One of these problems is related to the peculiarities of the behavior of the radial DWF near the origin of coordinates. Examples of this behavior are Refs. [3, 4], where the DWF contains a superfluous knot for one or both components in coordinate representation. There are two reasons for this inconsistency. The first reason is related to numerical inaccuracies for the determination of DWF when using certain program algorithms (codes) [5]. The second reason is related to the use of nucleon-nucleon interaction potentials.

Given these behavioral features for DWF, accurate studies for DWF can be performed near the origin of coordinates. By learning about the reliable information about asymptotics for DWFs or making the right fit for them, we can begin to calculate polarization characteristics for important processes, where the deuteron plays a key role as a target or incident

beam. For this purpose it is necessary to conduct modeling for DWF in coordinate representation using one potential of nucleon-nucleon interaction.

The purpose of this study is the modeling of DWF in coordinate representation with subsequent use to find polarization characteristics. In this case, the asymptotics near the origin of coordinates and at infinity must be taken into account for DWF. For a more correct and simplified task, we will use one nucleon-nucleon potential. It will be the potential Reid93 from the Nijmegen group [6, 7].

## 2. Deuteron wave function in coordinate representation

DWF as the main characteristic describes the deuteron as a quantum mechanical system. The knowledge of DWF allows us to obtain the maximum information about this coupled system for neutron and proton, as well as to theoretically calculate and predict those characteristics that depend on DWFs measured in the experiment.

In the theoretical description of DWF forms, such denominations [8] as “analytical form”, its “approximation” or “parameterization” are used in the coordinate representation. Often, the appellation “analytical form” is used as the resulting solution to the Schrödinger bound system. Later in the papers, this label is used to refer to records obtained as a result of the approximation for DWF.

In a detailed review [8] for the 1940-2015 years, the static parameters of deuteron, which were calculated by the DWF for various potentials and models, are systematized and described. The presence or absence of knots near the origin of coordinates for the radial DWF in coordinate representation is indicated. According to the references in the cited literature, an overview of analytical forms for DWFs was con-

ducted. In addition, the asymptotic behavior of the DWF near the origin of coordinates and for large distances is analyzed.

The analysis of the relationships for DWFs shows [8] that most analytical forms and parameterizations are presented in the form of exponential expansions.

Consider the DWF in coordinate representation in detail. When considering specific problems in order to determine the polarization characteristics, it is necessary to select the available DWFs in the literature or to find these functions independently. In the first case, researchers pay attention to the simple recording and convenient form of such DWF. In the second case, the DWF is calculated using the coupled system for Schrödinger equations and the nucleon-nucleon potential in the coordinate space. The obtained numerical values of DWFs are logical to represent in the form of visual, simple and convenient approximations.

After selecting the approximation dependence for the description of the DWF in coordinate representation, the model DWF should be analyzed. There are three steps to this end.

The first step is to find the difference between the numerical data and the approximation form. This difference is characterized by integrals [3] for the S- and D- states of the deuteron respectively

$$I_S = \left( \int_0^{\infty} [u_{approx}(r) - u_{table}(r)]^2 dr \right)^{1/2},$$

$$I_D = \left( \int_0^{\infty} [w_{approx}(r) - w_{table}(r)]^2 dr \right)^{1/2},$$

or by the magnitude of  $\chi^2$  corresponding to the degree of freedom

$$\chi^2 = \frac{1}{n-k} \sum_{i=1}^N (y_i - f(x_i; a_1, a_2, \dots, a_k))^2,$$

where  $n$  - the number of points of the array  $y_i$  of the numerical values of DWF in coordinate representation;  $f$  - approximating function for  $u(r)$  or  $w(r)$ ;  $a_1, a_2, \dots, a_k$  - parameters;  $k$  - the number of parameters.

The second step investigates the static parameters for the deuteron. The obtained DWF in the numerical calculations is tested for compliance with the theoretical values of deuteron static parameters and their experimental data. This is a must, since these static parameters are determined by DWF in coordinate representation [3, 9, 10]:

- the radius ("matter radius") of deuteron:

$$r_m = \frac{1}{2} \left\{ \int_0^{\infty} r^2 [u^2(r) + w^2(r)] dr \right\}^{1/2}; \quad (1)$$

- the electric quadrupole moment:

$$Q_d = \frac{1}{20} \int_0^{\infty} r^2 w(r) [\sqrt{8}u(r) - w(r)] dr$$

$$= \frac{1}{\sqrt{50}} \int_0^{\infty} r^2 \left[ u(r)w(r) - \frac{w^2(r)}{\sqrt{8}} \right] dr; \quad (2)$$

- the contribution of D-state:

$$P_D = \int_0^{\infty} w^2(r) dr; \quad (3)$$

- the magnetic moment:

$$\mu_d = \mu_s - \frac{3}{2} \left( \mu_s - \frac{1}{2} \right) P_D; \quad (4)$$

- the asymptotics of D/S- state:

$$\eta = A_D/A_S; \quad (5)$$

where  $A_S$  and  $A_D$  are the asymptotics of the normalization of the S- and D- state wave functions. The value  $\mu_s = \mu_n + \mu_p$  in Eq. (4) is the sum of the magnetic moments of the neutron and proton. The values of the deuteron magnetic moment are given in nuclear magnetons  $\mu_N$ .

Only after passing these three steps, the obtained DWF can be used to calculate the polarization observables in processes involving deuteron.

### 3. Superfluous knots of the deuteron wave function in coordinate representation

The calculated values of the static characteristics of the deuteron are in good agreement with the experimental data. However, there are some theoretical inconsistencies and problems. Thus, in some Refs., one (for example, for OBEP [11], Bonn [3] potentials) or both (for RSC [12], Moscow [4], renormalized chiral and [13] potentials) components for radial DWF have knots near the origin of coordinates. As noted earlier, this is also related to the features of the potential models for describing the deuteron. Next, we will look at the confirmation of this reason.

In [14] it was noted, that there is one coupled allowed state in the D- wave. This state together with the S- wave determines the ground state of the deuteron.

As noted in [15], the wave function for the S-wave in a deuteron is of the form 2 s and a knot at  $r \approx 0.5$  fm, which has the characteristics of a repulsive core characteristic of meson-exchange potentials. Due to the presence of color, this phenomenon cannot be conditioned by Pauli's exclusion principle for quark degrees of freedom.

In the context of chiral effective theory ( $\chi$ ET) [16], oscillations are available in the numerical integration of values  $\langle r^{-n} \rangle_{\Lambda}$ , which are associated with the appearance of erroneous coupled states whose bond energies exceed the scale

of partition  $1/\Lambda$ , where  $\Lambda$  is the scale at which the potential is regulated.

There are no knots for DWF in the coordinate representation for the Nijmegen group potentials [7], as well as for Argonne v14 and v18 [17], Paris [18] potentials.

#### 4. Polarization characteristics and the deuteron wave function

Among the large set of polarization characteristics in processes with the participation of deuteron [19], we choose such quantities that characterize two different processes. This is a tensor deuteron polarization  $t_{20}$  for elastic electron-deuteron scattering and a tensor analyzing power  $A_{yy}$  for inelastic scattering of deuterons (A(d,d')X reaction at light nuclei).

The first polarization characteristic of  $t_{20}$  is an important value because it is expressed through three deuteron form factors (FFs) and is determined by the experiment. At the same time, the magnitude of tensor polarization  $t_{20}$  is determined by the functions of structure  $A(p)$ ,  $B(p)$  and the scattering angle  $\theta$ . Tensor deuteron polarization  $t_{20}$  is represented as [1, 2, 20–22]

$$t_{20}(p, \theta_e) = -\frac{1}{\sqrt{2}S} \left( \frac{8}{3}\eta G_C(p)G_Q(p) + \frac{8}{9}\eta^2 G_Q^2(p) + \frac{1}{3}\eta \left[ 1 + 2(1 + \eta)tg^2 \left( \frac{\theta_e}{2} \right) \right] G_M^2(p) \right). \quad (6)$$

An alternative name for  $t_{20}$  is the tensor deuteron analyzing power [23, 24] and is often indicated to as  $T_{20}$ .

Here the factor  $S(p, \theta_e) = A(p) + B(p)tg^2(\theta_e/2)$  depends on electrical and magnetic structure functions of a deuteron [1, 2, 25]

$$A = G_C^2 + \frac{8}{9}\eta^2 G_Q^2 + \frac{2}{3}\eta G_M^2; \quad B = \frac{4}{3}\eta(1 + \eta)G_M^2. \quad (7)$$

Charge  $G_C(p)$ , quadrupole  $G_Q(p)$  and magnetic  $G_M(p)$  deuteron FFs contain information about the electromagnetic properties of a deuteron [2, 26]:

$$G_C = G_{EN}D_C, \quad G_Q = G_{EN}D_Q, \\ G_M = \frac{m_d}{2m_p} (G_{MN}D_M + G_{EN}D_E). \quad (8)$$

Here, the “body factors”  $D_i$  are determined by the DWF in the coordinate representation  $u(r)$  and  $w(r)$ :

monopole electric

$$D_C = \int_0^\infty [u^2 + w^2] j_0 dr;$$

quadrupole electric

$$D_Q = \frac{3}{\sqrt{2}\eta} \int_0^\infty \left[ uw - \frac{w^2}{\sqrt{8}} \right] j_2 dr;$$

transverse magnetic

$$D_M = 2 \int_0^\infty \left[ \left( u^2 - \frac{w^2}{2} \right) j_0 + \left( \frac{uw}{\sqrt{2}} + \frac{w^2}{2} \right) j_2 \right] dr;$$

longitudinal magnetic

$$D_E = \frac{3}{2} \int_0^\infty w^2 [j_0 + j_2] dr.$$

Here  $G_{EN} = G_{Ep} + G_{En}$ ;  $G_{MN} = G_{Mp} + G_{Mn}$  are the isoscalar electric and magnetic FFs;  $G_{Ep}$  and  $G_{En}$  are proton and neutron isoscalar electric FFs;  $G_{Mp}$  and  $G_{Mn}$  are proton and neutron isoscalar magnetic FFs;  $j_0, j_2$  are spherical Bessel functions of zero and second order from argument  $pr/2$ . The dipole form was used for electromagnetic nucleon form factors.

Experimental data for tensor deuteron polarization  $t_{20}(p)$  are given in the Refs. of Bates [21, 27, 28], JLab [22, 29], VEPP-3 [30–34], NIKHEF [35, 36], Saclay [37], BLAST [23, 24, 38] collaborations and in Boden [39], Garcon [21], Abbott [40] reviews.

To estimate the tensor analyzing power  $A_{yy}$  as the polarization observables in the A(d,d')X reaction, we can use the models of plane wave impulse approximation (PWIA) [41] and  $\omega$ -meson exchange [42, 43].

The magnitude of the tensor analyzing power  $A_{yy}$  can be experimentally obtained from the numbers of deuterons  $n^+$ ,  $n^-$ ,  $n^0$ , which registered for different modes of beam polarization  $p_z, p_{zz}$ , and normalized to the beam intensity, taking into account the effect of dead installation time [44]:

$$A_{yy} = 2 \frac{p_z^-(n^+/n^0 - 1) - p_z^+(n^-/n^0 - 1)}{p_z^- p_{zz}^+ - p_z^+ p_{zz}^-}. \quad (9)$$

Tensor analyzing power in PWIA is theoretically calculated by the following formula [41]:

$$A_{yy} = \frac{T_{00}^2 - T_{11}^2 + 4P^2 T_{10}^2}{T_{00}^2 + 2T_{11}^2 + 4P^2 T_{10}^2}, \quad (10)$$

where  $T_{ij}(p/2)$  are the amplitudes, which are determined by the radial DWF in the coordinate representation  $u(r)$  and  $w(r)$ :

$$T_{00} = S_0 + \sqrt{2}S_2, \quad T_{11} = S_0 - \frac{1}{\sqrt{2}}S_2, \quad (11)$$

$$T_{10} = \frac{i}{\sqrt{2}} \int_0^\infty \left( u^2 - \frac{w^2}{2} \right) j_0 dr \\ + \frac{i}{2} \int_0^\infty w \left( u + \frac{w}{\sqrt{2}} \right) j_2 dr. \quad (12)$$

Here,  $S_0$  and  $S_2$  are the spherical (charge) and quadrupole FFs of the deuteron

$$\begin{aligned} S_0(p/2) &= S_0^{(1)} + S_0^{(2)}, \\ S_2(p/2) &= 2S_2^{(1)} - \frac{1}{\sqrt{2}}S_2^{(2)}, \end{aligned} \quad (13)$$

expressed through spherical  $S_0^{(i)}$  and quadrupole  $S_2^{(i)}$  FFs [41, 45]

$$\begin{aligned} S_0^{(1)} &= \int_0^\infty u^2 j_0 dr, & S_0^{(2)} &= \int_0^\infty w^2 j_0 dr, \\ S_2^{(1)} &= \int_0^\infty uw j_2 dr, & S_2^{(2)} &= \int_0^\infty w^2 j_2 dr. \end{aligned} \quad (14)$$

In Eq. (10), the parameter  $P = a \cdot p$  at  $a = 0.4$  [41] is used.

The experimental data for the tensor analyzing power  $A_{yy}$  are given for the reaction of type (d,d') on light nuclei: on hydrogen [46], carbon [46–48], beryllium [42–44]. From the data of [48] the tensor analyzing ability is determined by the formula:  $A_{yy} = -T_{20}/\sqrt{2}$ .

It is better to calculate those polarization characteristics that are sufficiently defined in the experiment. Then, we can compare theoretical calculations with experimental data over a wide range of transmitted momentums. As a consequence, the conclusion of model calculations and the satisfaction of a particular potential model for experiment will be fully justified.

## 5. Calculations and results

Numerical calculations show that a certain number of additions to the expansion sums for DWF in coordinate representation will show a superfluous knot near the origin of coordinates. More often this effect is present at small number of additives. To eliminate this effect, it is necessary to increase the number of additions in the sum of the expansions. However, this can lead to large rounding errors.

The second feature of the calculations for DWF in the coordinate representation is its form of asymptotics at  $r \rightarrow 0$  and at  $r \rightarrow \infty$ . Among the list of asymptotics at  $r \rightarrow 0$  we pay attention to the following:

1) in Ref. [49]

$$u(r) \rightarrow r, \quad w(r) \rightarrow r^3, \quad (15)$$

2) in Ref. [50]

$$u(r) \rightarrow r^2, \quad w(r) \rightarrow r^3. \quad (16)$$

The standard asymptotics for DWF as  $r \rightarrow \infty$  is this representation [49]

$$\begin{aligned} u(r) &\sim A_S \exp(-\beta r), \\ w(r) &\sim A_D \exp(-\beta r) \left[ 1 + \frac{3}{\beta r} + \frac{3}{(\beta r)^2} \right], \end{aligned} \quad (17)$$

where  $\beta = \sqrt{ME_d}$ ;  $M$  is the nucleon mass;  $E_d$  is the binding energy of the deuteron.

To approximate the DWF in coordinate representation for Reid93 potential, we use the following forms [51, 52]

$$\begin{cases} u(r) = r \sum_{i=1}^N A_i \exp(-a_i r), \\ w(r) = r^2 \sum_{i=1}^N B_i \exp(-b_i r). \end{cases} \quad (18)$$

The degrees for  $r^n$  before the sums of the expansions were chosen optimal so that the obtained DWF satisfies the static parameters.

Application of the approximation to DWF for Reid93 potential by the formulas [51, 53]

$$\begin{cases} u(r) = \sum_{n=0}^{\infty} c_n \psi_{1n}(r), \\ w(r) = \sum_{n=0}^{\infty} d_n \psi_{1n}(r). \end{cases} \quad (19)$$

does not cause the knot to appear only in the component  $u(r)$ . Here  $\psi_{1n}(r)$  - Laguerre functions [51]:

$$\begin{aligned} \psi_{1n}(r) &= \frac{\sqrt{2\alpha}}{n!} \exp(\alpha r) \\ &\times \frac{d^n}{dr^n} (r^n \exp(-2\alpha r)), \quad n = 0, 1, 2, 3, \dots \end{aligned}$$

Figures 1 and 2, also show the DWFs for OBEPB [54] and fss2 [55] models for qualitative comparison. The indicated DWF behavior near the origin of coordinates indicates the numerical problems of the calculations.

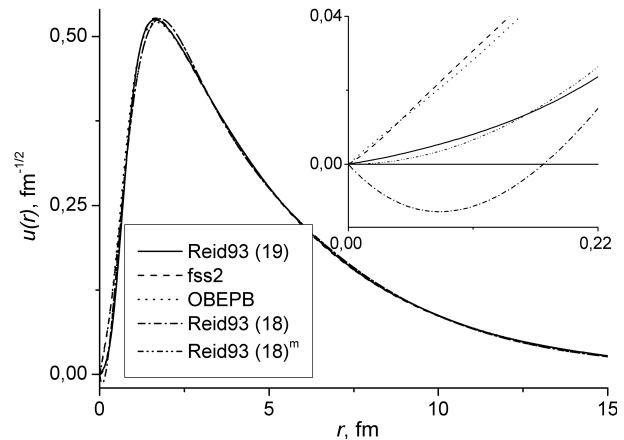


FIGURE 1. The wave function  $u(r)$  for various potentials, as function of coordinate  $r$ .

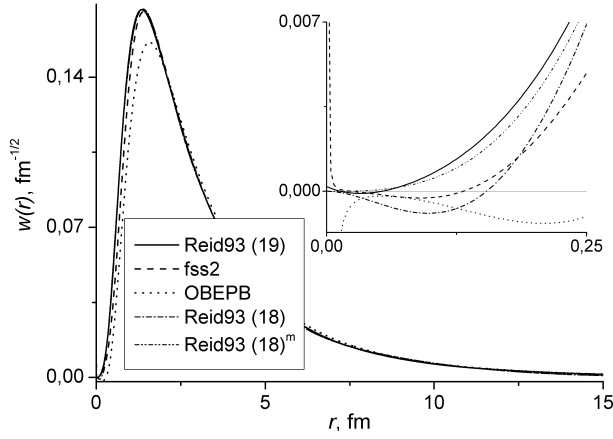


FIGURE 2. The wave function  $w(r)$  for various potentials, as function of coordinate  $r$ .

Without going into the details of obtaining these asymptotics (16) and (17), we apply them to our model representations of DWFs. The submission area for DWF was actually divided into three parts:

- 1)  $0 - 0.301$  fm,
- 2)  $0.301 - 24.997$  fm, 3)  $24.997$  fm  $-\infty$ . (20)

The reason for this division into three regions below is explained by the peculiarities of the numerical calculations for (18).

In numerical calculations of DWF for potential Reid93 by formulas (18), a superfluous knot was found at  $r = 0.172$  fm and  $0.154$  fm for the components  $u(r)$  and  $w(r)$ , respectively (Figs. 1 and 2). This superfluous knot near the origin of coordinates is prevented by approximation. For example, you can use the approximation in the form (16) [50] to coordinate values  $r = 0.301$  fm. The asymptotic behavior of DWFs as  $r \rightarrow \infty$  is chosen as (17). In Figs. 1 and 2, this DWF modification is designated (18)<sup>m</sup>.

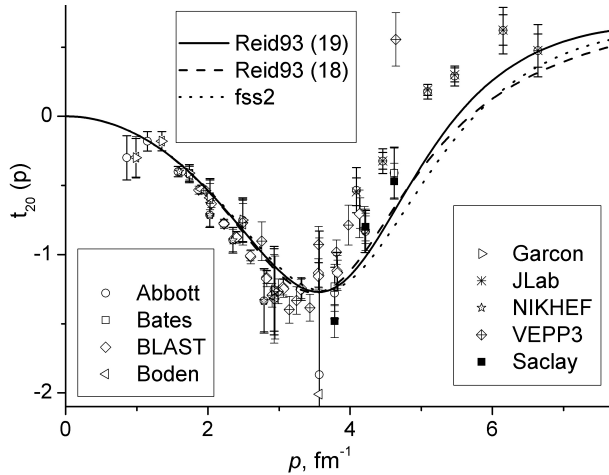


FIGURE 3. The tensor deuteron polarization  $t_{20}$ , as function of transmitted momentum  $p$ . The experimental data are taken from Refs. [21–24, 27–40].

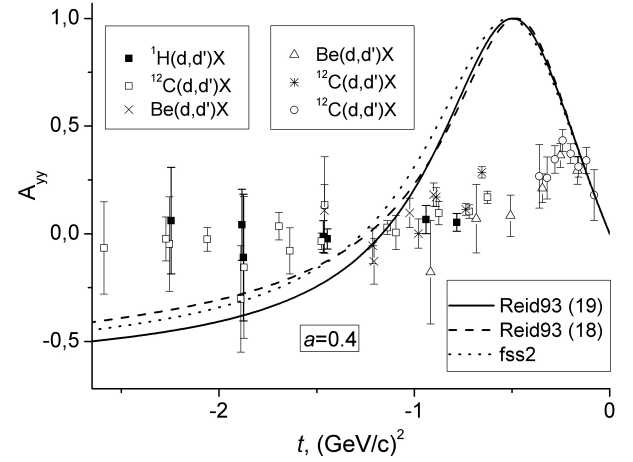


FIGURE 4. The tensor analyzing power  $A_{yy}$ , as function of transmitted momentum  $p$ . The experimental data are taken from Refs. [42–44, 46–48].

In Figs. 3 and 4 present the results of calculations of the polarization characteristics of  $t_{20}$  and  $A_{yy}$  for the model calculations for the DWF for Reid93 potential by (18). The optimal number of additions in (19) for Reid93 potential is  $n = 17$ . The difference between these calculations is due to different expansions and high-momentum component. The theoretical values obtained are compared with the experimental data. In Fig. 4 uses  $t$ -scaling according to the elementary notation by the formula  $t = -(0.197326p)^2$  at the units for momentum  $p$  in [ $\text{fm}^{-1}$ ] and  $t$ -scaling in [ $(\text{GeV}/c)^2$ ].

For the polarization characteristic  $A_{yy}$ , the difference between theoretical calculations and experimental data (for  $N_{\text{data}}=45$  values) is described by  $\chi^2/N_{\text{data}}$ , which is equal to 0.159425, 0.132223 and 0.153614 for DWFs for the potentials fss2, Reid93 (18) and Reid93 (19), respectively. Similarly for the characteristic  $t_{20}$  (at  $N_{\text{data}}=96$ ), these values are given as 0.090236, 0.067306 and 0.068475. The smaller the deviation  $\chi^2/N_{\text{data}}$ , the better the theory describes the experiment in a given region of transmitted momentums. That is, the theoretical calculations with DWF for the Reid93 potential by (18) are better consistent with the experiment.

Figure 5 compares the results of  $t_{20}$  for the approximation (18) for potential Reid93. It takes into account the peculiarities of the DWF behavior at different coordinate regions according to (20). Purely calculations for (18) are designated as “DWF (18)”. The refinement of the asymptotics to  $r = 0.301$  fm by the formula (16) is denoted as “DWF (18) + asymp. (16)”. If we consider asymptotics (17) after the coordinate point  $r = 24.997$  fm in the previous case, then we have the calculations “DWF (18) + asymp. (16) + (17)”.

As the analysis of the results for  $t_{20}$  shows, the difference between the calculations slightly depends on the specification of the asymptotic behavior of the DWF in the coordinate representation. Refinements of DWFs were compared with each other using the ratio of polarization characteristics. Ratio of “DWF (18)” / “DWF (18) + asymp. (16)” and “DWF (18)” / “DWF (18) + asymp. (16) + (17)” were the same. This

TABLE I. Theoretical and experimental values of deuteron parameters: D- state contribution  $P_D$ , matter radius  $r_m$ , electric quadrupole moment  $Q_d$ , magnetic moment  $\mu_d$ , the asymptotics of D/S- state  $\eta$ .

Potential	$P_D$ [%]	$r_m$ [fm]	$Q_d$ [fm <sup>2</sup> ]	$\mu_d$ [ $\mu_N$ ]	$\eta$
Reid 93, DWF (18); $N=17$	5.6948	1.9694	0.26703	0.847356	0.02477
Reid 93, DWF (18)+ asymp. (16); $N=17$	5.6949	1.9694	0.26703	0.847356	0.02477
Reid 93, DWF (18)+ asymp. (16) + (17); $N=17$	5.6949	1.9689	0.26703	0.847356	0.02477
Reid 93 (19); $n=17$	5.6992	1.9677	0.27019	0.847332	0.02458
Reid 93 (19) [53]	5.7009	1.9671	0.27015	0.847322	0.02426
Reid 93 [6, 56]	5.699	1.969	0.2703	-	0.0251
Nijm I [6, 56]	5.664	1.967	0.2719	-	0.0253
Nijm II [6, 56]	5.635	1.968	0.2707	-	0.0252
Nijm 93 [6, 56]	5.755	1.966	0.2706	-	0.0252
Argonne v18 [17]	5.76	1.967	0.270	0.847	0.0250
Experiment [1]	-	1.975(3)	0.2859(3)	0.857438	0.0256(4)

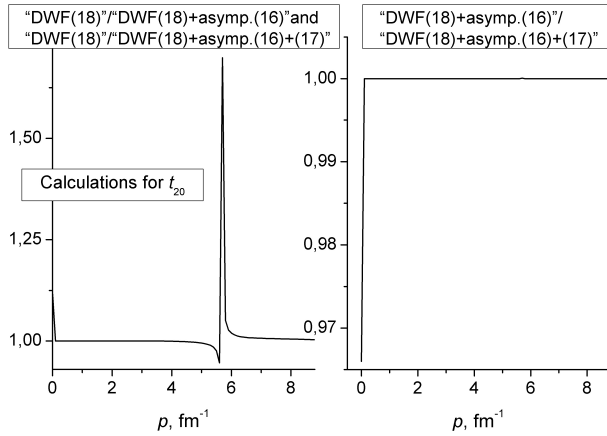


FIGURE 5. Comparison of the results of  $t_{20}$  for approximation (18) taking into account asymptotics.

means that it is not possible to find out the difference between the asymptotics of DWF. Therefore, it is necessary to find a direct numerical difference between the results of the refinements of the asymptotics, that is, the ratio of the results “DWF (18) + asymp. (16)” and “DWF (18) + asymp. (16) + (17)”. The influence of “manual recording” of asymptotics in the calculations of the tensor analyzing power  $A_{yy}$  was similarly evaluated.

As can be seen from Figs. 5 and 6 there is only a slight difference in the calculations in the narrow region of the transmitted momentums. What is the reason for the difference between calculations in a small region? Obviously, we need to turn to the algorithm of numerical calculation. The peculiarity of determining the polarization characteristics is that they contain mathematical expressions with spherical Bessel functions of zero and second order. These functions are in integrals ranging from zero to infinity (formulas for elementary “body form factors” and form factors (14)).

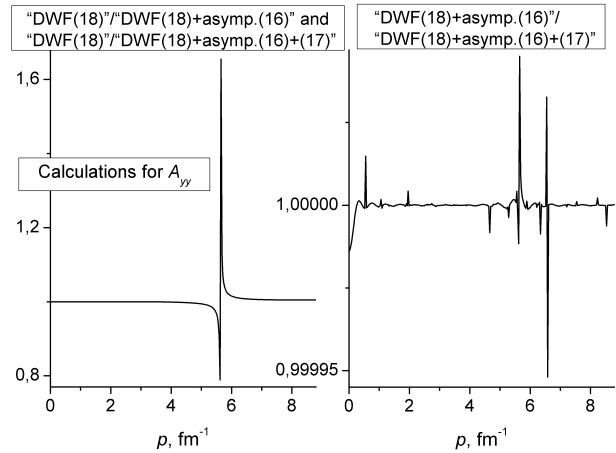


FIGURE 6. Comparison of the results of  $A_{yy}$  for approximation (18) taking into account asymptotics.

In general, such meticulous refinements do not affect the overall appearance of the polarization characteristics. The insignificant difference between the calculations with the choice of different asymptotics does not affect the general behavior in the scale of the transmitted momentums. However, the analysis of numerical data is fully justified. And such numerical refinements based on asymptotics for DWF may be useful for further refinements for a specific accurate momentum value or for a narrow momentum interval.

The static parameters of the deuteron are shown in Table I. The data obtained are compared with the results of theoretical calculations in other studies and experimental values. The difference between them is not significant.

## 6. Conclusions

1. The simulation for DWF in coordinate representation for the nucleon-nucleon potential Reid93 is performed. For this purpose, we take into account the asymptotics

of the radial DWF near the origin of coordinates and at infinity. Such asymptotics, which are the most simple and physical, are applied.

2. Compensated superfluous knots for both DWF components in coordinate representation to the coordinate value  $r=0.301$  fm are illustrated.
3. On the basis of the obtained DWFs in the coordinate

representation, two polarization characteristics of  $t_{20}$  and  $A_{yy}$  were calculated. Taking into account the asymptotics of the wave function has little effect on the general behavior of these polarization characteristics. Particular points of the transmitted momentum have been identified, where the tensor deuteron polarization  $t_{20}$  and the tensor analyzing power  $A_{yy}$  show a clear difference.

- 
1. M. Garçon and J. W. Van Orden, The Deuteron: Structure and Form Factors, in *Advances in Nuclear Physics*, edited by J. W. Negele and E. W. Vogt (Springer, Boston, 2001), **Vol. 26**, Chap. 4, [https://doi.org/10.1007/0-306-47915-X\\_4](https://doi.org/10.1007/0-306-47915-X_4).
  2. R. Gilman and F. Gross, *Electromagnetic structure of the deuteron*, *J. Phys. G* **28** (2002) R37, <https://doi.org/10.1088/0954-3899/28/4/201>.
  3. R. Machleidt, *High-precision, charge-dependent Bonn nucleon-nucleon potential*, *Phys. Rev. C* **63** (2001) 024001, <https://doi.org/10.1103/PhysRevC.63.024001>.
  4. V. I. Kukulín, *Moscow-type NN potentials and three-nucleon bound states*, *Phys. Rev. C* **57** (1998) 535, <https://doi.org/10.1103/PhysRevC.57.535>.
  5. I. Haysak and V. Zhaba, *On the nodes of the deuteron wave function*, *Visnyk Lviv Univ. Ser. Phys.* **44** (2009) 8.
  6. V. G. J. Stoks, R. A. M. Klomp, C. P. F. Terheggen, and J. J. de Swart, *Construction of high-quality NN potential models*, *Phys. Rev. C* **49** (1994) 2950, <https://doi.org/10.1103/PhysRevC.49.2950>.
  7. J. J. de Swart, R. A. M. Klomp, M. C. M. Rentmeester, and T. A. Rijken, *The Nijmegen potentials*, *Few Body Syst. Suppl.* **8** (1995) 438.
  8. V. I. Zhaba, *Deuteron: properties and analytical forms of wave function in coordinate space*, e-print arXiv:nucl-th/1706.08306 (2017).
  9. J. M. Blatt and V. F. Weisskopf, *Theoretical Nuclear Physics* (Springer, New York, 1979), <https://doi.org/10.1007/978-1-4612-9959-2>.
  10. S. De Benedetti, *Nuclear Interactions* (John Wiley and Sons, New York, 1964).
  11. R. Machleidt, K. Holinde, and Ch. Elster, *The Bonn meson-exchange model for the nucleon-nucleon interaction*, *Phys. Rep.* **149** (1987) 1, [https://doi.org/10.1016/S0370-1573\(87\)80002-9](https://doi.org/10.1016/S0370-1573(87)80002-9).
  12. R. V. Reid Jr., *Local phenomenological nucleon-nucleon potentials*, *Ann. Phys.* **50** (1968) 411, [https://doi.org/10.1016/0003-4916\(68\)90126-7](https://doi.org/10.1016/0003-4916(68)90126-7).
  13. E. Ruiz Arriola and M. Pavon Valderrama, *Deuteron radial moments for renormalized chiral potentials*, *Eur. Phys. J. A* **31** (2007) 549, <https://doi.org/10.1140/epja/i2006-10294-2>.
  14. S. B. Dubovichenko, *Properties of Light Atomic Nuclei in the Potential Cluster Model* (Daneker, Almaty, 2004).
  15. V. A. Knyr, V. G. Neudatchin, and N. A. Khokhlov, *Relativistic optical model on the basis of the Moscow potential and lower phase shifts for nucleon-nucleon scattering at laboratory energies of up to 3 GeV*, *Phys. At. Nucl.* **69** (2006) 2034, <https://doi.org/10.1134/S1063778806120064>.
  16. L. Platter and D. R. Phillips, *Deuteron matrix elements in chiral effective theory at leading order*, *Phys. Lett. B* **641** (2006) 164, <https://doi.org/10.1016/j.physletb.2006.08.053>.
  17. R. B. Wiringa, V. G. J. Stoks, and R. Schiavilla, *Accurate nucleon-nucleon potential with charge-independence breaking*, *Phys. Rev. C* **51** (1995) 38, <https://doi.org/10.1103/PhysRevC.51.38>.
  18. M. Lacombe *et al.*, *Parametrization of the Paris N - N potential*, *Phys. Rev. C* **21** (1980) 861, <https://doi.org/10.1103/PhysRevC.21.861>.
  19. G. G. Ohlsen, *Polarization transfer and spin correlation experiments in nuclear physics*, *Rep. Prog. Phys.* **35** (1972) 717, <https://doi.org/10.1088/0034-4885/35/2/305>.
  20. R. G. Arnold, C. E. Carlson, and F. Gross, *Polarization transfer in elastic electron scattering from nucleons and deuterons*, *Phys. Rev. C* **23** (1981) 363, <https://doi.org/10.1103/PhysRevC.23.363>.
  21. M. Garçon *et al.*, *Tensor polarization in elastic electron-deuteron scattering in the momentum transfer range  $3.8 \leq Q \leq 4.6 \text{ fm}^{-1}$* , *Phys. Rev. C* **49** (1994) 2516, <https://doi.org/10.1103/PhysRevC.49.2516>.
  22. D. Abbott *et al.* (The Jefferson Lab t20 Collaboration), *Measurement of Tensor Polarization in Elastic Electron-Deuteron Scattering at Large Momentum Transfer*, *Phys. Rev. Lett.* **84** (2000) 5053, <https://doi.org/10.1103/PhysRevLett.84.5053>.
  23. C. Zhang *et al.* (The BLAST Collaboration), *Precise Measurement of Deuteron Tensor Analyzing Powers with BLAST*, *Phys. Rev. Lett.* **107** (2011) 252501, <https://doi.org/10.1103/PhysRevLett.107.252501>.
  24. D. K. Hasell *et al.*, *Spin-Dependent Electron Scattering from Polarized Protons and Deuterons with the BLAST Experiment at MIT-Bates*, *Annu. Rev. Nucl. Part. Sci.* **61** (2011) 409, <https://doi.org/10.1146/annurev-nucl-100809-131956>.

25. T. W. Donnelly and A. S. Raskin, *Considerations of polarization in inclusive electron scattering from nuclei*, *Ann. Phys.* **169** (1986) 247, [https://doi.org/10.1016/0003-4916\(86\)90173-9](https://doi.org/10.1016/0003-4916(86)90173-9).
26. M. Gourdin, *Deuteron electromagnetic form factors*, *Nuovo Cimento* **28** (1963) 533, <https://doi.org/10.1007/BF02828871>.
27. M. E. Schulze *et al.*, *Measurement of the Tensor Polarization in Electron-Deuteron Elastic Scattering*, *Phys. Rev. Lett.* **52** (1984) 597, <https://doi.org/10.1103/PhysRevLett.52.597>.
28. I. The *et al.*, *Measurement of tensor polarization in elastic electron-deuteron scattering in the momentum-transfer range  $3.8 \leq q \leq 4.6 \text{ fm}^{-1}$* , *Phys. Rev. Lett.* **67** (1991) 173, <https://doi.org/10.1103/PhysRevLett.67.173>.
29. S. Kox *et al.* (The Jefferson Lab t20 Collaboration), *Measurement of tensor polarization in elastic electron-deuteron scattering at large momentum transfer*, *Nucl. Phys. A* **684** (2001) 521, [https://doi.org/10.1016/S0375-9474\(01\)00370-0](https://doi.org/10.1016/S0375-9474(01)00370-0).
30. R. Gilman *et al.*, *Measurement of tensor analyzing power in electron-deuteron elastic scattering*, *Phys. Rev. Lett.* **65** (1990) 1733, <https://doi.org/10.1103/PhysRevLett.65.1733>.
31. D. M. Nikolenko *et al.*, *Measurement of polarization observables in elastic and inelastic electron-deuteron scattering at the VEPP-3 storage ring*, *Nucl. Phys. A* **684** (2001) 525, [https://doi.org/10.1016/S0375-9474\(01\)00373-6](https://doi.org/10.1016/S0375-9474(01)00373-6).
32. D. M. Nikolenko *et al.*, *Measurement of the Tensor Analyzing Powers  $T_{20}$  and  $T_{21}$  in Elastic Electron-Deuteron Scattering*, *Phys. Rev. Lett.* **90** (2003) 072501, <https://doi.org/10.1103/PhysRevLett.90.072501>.
33. D. M. Nikolenko *et al.*, *Experiments with internal targets at the VEPP-3 electron storage ring*, *Phys. At. Nucl.* **73** (2010) 1322, <https://doi.org/10.1134/S1063778810080065>.
34. S. A. Zevakov *et al.*, *Elastic and inelastic electron scattering on tensor polarised deuteron*, Preprint IJD 2006-024, Novosibirsk, 2006.
35. M. Ferro-Luzzi *et al.*, *Measurement of Tensor Analyzing Powers for Elastic Electron Scattering from a Polarized  $^2\text{H}$  Target Internal to a Storage Ring*, *Phys. Rev. Lett.* **77** (1996) 2630, <https://doi.org/10.1103/PhysRevLett.77.2630>.
36. M. Bouwuis *et al.*, *Measurement of  $T_{20}$  in Elastic Electron-Deuteron Scattering*, *Phys. Rev. Lett.* **82** (1999) 3755, <https://doi.org/10.1103/PhysRevLett.82.3755>.
37. B. Frois, *Electron-nucleus interactions (Part 3)*, *Nucl. Phys. A* **527** (1991) 357, [https://doi.org/10.1016/0375-9474\(91\)90125-P](https://doi.org/10.1016/0375-9474(91)90125-P).
38. M. Kohl, *Elastic Form Factors of the Proton, Neutron and Deuteron*, *Nucl. Phys. A* **805** (2008) 361c, <https://doi.org/10.1016/j.nuclphysa.2008.02.276>.
39. B. Boden *et al.*, *Elastic electron deuteron scattering on a tensor polarized solid  $\text{ND}_3$  target*, *Z. Phys. C* **49** (1991) 175, <https://doi.org/10.1007/BF01555492>.
40. D. Abbott *et al.*, *Phenomenology of the deuteron electromagnetic form factors*, *Eur. Phys. J. A* **7** (2000) 421, <https://doi.org/10.1007/PL00013629>.
41. V. P. Ladygin and N. B. Ladygina, *Polarization effects in inelastic deuteron scattering in the region of baryon-resonance excitation*, *Phys. At. Nucl.* **65** (2002) 182, <https://doi.org/10.1134/1.1446569>.
42. V. P. Ladygin *et al.*, *Measurement of the tensor analyzing power  $A_{yy}$  in the inelastic scattering of deuterons in the vicinity of excitation of baryonic resonances*, *Eur. Phys. J. A* **8** (2000) 409, <https://doi.org/10.1007/s100500070095>.
43. L. S. Azhgirey *et al.*, *Measurement of the tensor analyzing power  $A_{yy}$  in the inelastic scattering of 4.5-GeV/c deuterons on beryllium at an angle of 80 mrad*, *Phys. At. Nucl.* **64** (2001) 1961, <https://doi.org/10.1134/1.1423746>.
44. L. S. Azhgirey *et al.*, *Measurement of the tensor  $A_{yy}$  and vector  $A_y$  analyzing powers of the deuteron inelastic scattering of beryllium at 5.0 GeV/c and 178 mrad*, *Phys. At. Nucl.* **68** (2005) 991, <https://doi.org/10.1134/1.1954825>.
45. M. N. Patonova and V. I. Kukulín, *Refined Glauber model versus Faddeev calculations and experimental data for  $pd$  spin observables*, *Phys. Rev. C* **81** (2010) 014004, <https://doi.org/10.1103/PhysRevC.81.014004>.
46. V. P. Ladygin *et al.*, *Tensor  $A_{yy}$  and vector  $A_y$  analyzing powers in the  $^1\text{H}(d, d')X$  and  $^{12}\text{C}(d, d')X$  reactions at initial deuteron momenta of 9 GeV/c in the region of baryonic resonance excitation*, *Phys. At. Nucl.* **69** (2006) 852, <https://doi.org/10.1134/S1063778806050073>.
47. S. V. Afanasiev *et al.*, *Tensor and Vector Analysing Powers  $A_{yy}$  and  $A_y$  in the  $^{12}\text{C}(d, p)X$  and  $^{12}\text{C}(d, d)X$  Reactions at Initial Deuteron Momentum of 9 GeV/c and Emission Angle of 85 mrad*, *JINR Rapid Commun.* **2[88]-98**, 5.
48. L. S. Azhgirey *et al.*, *Tensor Analysing Power  $T_{20}$  in Inelastic  $(d, d')X$  Scattering at  $0^\circ$  on  $^1\text{H}$  and  $^{12}\text{C}$  from 4.5 to 9.0 GeV/c*, *JINR Rapid Commun.* **2[88]-98**, 17.
49. M. Lacombe *et al.*, *Parametrization of the deuteron wave function of the Paris  $N - N$  potential*, *Phys. Lett. B* **101** (1981) 139, [https://doi.org/10.1016/0370-2693\(81\)90659-6](https://doi.org/10.1016/0370-2693(81)90659-6).
50. Yu. A. Berezhnoy, V. Yu. Korda, and A. G. Gakh, *Matter-Density Distribution in Deuteron and Diffraction Deuteron-Nucleus Interaction*, *Int. J. Mod. Phys. E* **14** (2005) 1073, <https://doi.org/10.1142/S0218301305003697>.
51. F. Cap and W. Gröbner, *New Method for the Solution of the Deuteron Problem, and its Application to a Regular Potential*, *Nuovo Cimento* **1** (1955) 1211, <https://doi.org/10.1007/BF02731424>.
52. V. I. Zhaba, *Analytical Forms of the Wave Function in Coordinate Space and Tensor Polarization of the Deuteron for Potentials Nijmegen Group*, *J. Phys. Stud.* **20** (2016) 3101, <https://doi.org/10.30970/jps.20.3101>.
53. V. I. Zhaba, *New Analytical Forms Through Laguerre Functions for Wave Function in Coordinate Space and Tensor Polarization of Deuteron*, *Electron. J. Theor. Phys.* **13** (2016) 147.
54. R. Machleidt, *The Meson Theory of Nuclear Forces and Nuclear Structure*, in *Advances in Nuclear Physics*, edited

- by J. W. Negele and E. W. Vogt (Springer, Boston, 1989), Vol. 19, Chap. 2, [https://doi.org/10.1007/978-1-4613-9907-0\\_2](https://doi.org/10.1007/978-1-4613-9907-0_2).
55. Y. Fujiwara *et al.*, *Resonating-group study of baryon-baryon interactions for the complete baryon octet: NN interaction*, Phys. Rev. C **65** (2001) 014002, <https://doi.org/10.1103/PhysRevC.65.014002>.
56. NN-OnLine, NN interaction, <http://nn-online.org/NN/>.